

Two-scale model for aggregation and etching

George C. John

Physics Department, Indian Institute of Technology, Kanpur, Uttar Pradesh 208016, India

Vijay A. Singh*

Solid State Electronics Group, Tata Institute of Fundamental Research, Bombay 400 005, India

(Received 12 September 1995)

We propose a dual scale drift-diffusion model for interfacial growth and etching processes. The two scales are (i) a depletion layer width ΔW surrounding the aggregate, and (ii) a drift length l . The interplay between these two antithetical scales yields a variety of distinct morphologies reported in electrochemical deposition of metals, in viscous fingering in fluids, and in porous silicon formation. Further, our algorithm interpolates between existing growth models (diffusion limited aggregation, ballistic deposition, and Eden) for limiting values of ΔW and l .

PACS number(s): 61.43.Hv, 81.10.Aj, 68.70.+w, 81.65.-b

I. INTRODUCTION

The study of complex patterns in dimension $d = 2$ has attracted a great deal of attention in the past decade and a half. Systematic studies of emergent patterns in electrochemical deposition (ECD) of metals and of the morphologies obtained during fluid-fluid displacement in a Hele-Shaw setup have been carried out [1]. On the other hand, complex pore geometries of anodically etched silicon have also evoked considerable interest, on account of the technological promise of porous silicon [2]. A simple model that would describe the fascinating varieties of morphologies obtained both in aggregation and dissolution would be a desirable objective.

In electrochemical deposition experiments, two parameters, the electrolyte concentration (C) and the applied potential (V) are tuned to obtain (i) dendritic structures, both thick and needlelike (or stringy), (ii) dense branching morphologies, which are homogeneous, and (iii) randomly ramified self-similar structures as in diffusion limited aggregation (DLA) [3,4]. In a Hele-Shaw cell, similar transitions are observed when the pressure and surface tension are varied [1]. In silicon, anodic etching gives rise to differing pore morphologies depending on the anodization potential and the substrate doping level [2,5].

A first principles explanation of such phenomena will have to encompass (i) the diffusive field, (ii) the Laplace field, (iii) convective processes, and (iv) surface tension, curvature, and underlying anisotropy effects. Hence, even numerical solutions may prove difficult. Simple formal approaches have been attempted for obtaining stability conditions at the interface [6–8]. It has also been hypothesized that the emergence of different characterizing length scales is the result of the interplay between

the Laplace and diffusion fields governing the growth process in ECD [8]. Similar models have been proposed to model the anodic etching of silicon in hydrofluoric acid. A phenomenological Schottky diode model for porous silicon formation [5] invokes a depletion layer width at the interface with a substantial barrier lowering at the pore tips.

On the other hand, a simple algorithmic approach has been adopted in the last decade and a half to successfully capture the basic patterns mentioned above [9–11]. The most common among these is DLA [12], which results in a self-similar structure resembling zinc leaves grown in an electrolyte under certain limiting conditions. Generalizations of the DLA have been proposed by the introduction of additional parameters into the model. Surface tension effects have been modeled by the incorporation of a sticking probability at the aggregate surface [13]. This resulted in a transition from the low density fractal clusters to regular patterns. Recently, a multiwalker DLA model has been proposed [14] wherein two parameters, namely, the particle concentration and the width of a “migrational envelope” are tuned to obtain dense branching morphologies as well as DLA patterns.

In this paper, we propose a single walker, two parameter drift-diffusion model to simulate growth (and dissolution) in a wide variety of systems. Section II states the algorithm employed in the growth process. Section III summarizes the various growth patterns obtained in the simulations with differing parameters and correlates them to the morphological classes reported in experimental literature. Section IV constitutes a brief discussion.

II. THE DRIFT-DIFFUSION MODEL

It will be a desirable goal to arrive at a model that can reproduce the various morphologies obtained from different growth phenomena. Modeling the transition from one class of patterns to another will also be an interesting objective. Such transitions can be represented as

*Permanent address: Department of Physics, Indian Institute of Technology, Kanpur, India.

resulting from the interplay of two or more parameters [15,16]. Different morphologies result in the various limiting cases. However, to maintain the simplicity of such an approach, a minimal set of parameters should be employed.

In the classical DLA model [12], a particle starts its random walk at an infinitely large distance away from a seed or cluster. Its random diffusive motion is terminated the moment it comes into contact with the aggregate cluster. This simulation models diffusion in the low concentration limit and does not employ any control parameters. To control the diffusive process, the introduction of other variables such as a diffusion length [17,18] or particle concentration [19] have been suggested in the literature.

It is conceivable that very close to the aggregate surface, the particle movement is no longer controlled by the macroscopic diffusion field, but by microscopic, localized phenomena. To model such processes, additional parameters will have to be introduced into the simulation. We attempt to develop an algorithm that models pattern formation as a result of the interplay of a macroscopic field and localized surface phenomena.

The main control parameters in this model are (i) a depletion layer width ΔW that controls the diffusion and (ii) a drift length l governing the field driven processes in the proximity of the aggregate. The design of the algorithm is outlined below:

(i) The particles are launched, one at a time, from a randomly chosen lattice site beyond the depletion layer boundary at a distance ΔW from the surface of the aggregate. This is illustrated in Fig. 1. We begin with a circular depletion zone of radius ΔW around a central seed. As the aggregate grows, the depletion zone boundary is modified to follow the aggregate contour at a distance ΔW as shown in the figure. (ii) The particles execute random walks as in ordinary off-lattice DLA algorithms [10,20]. (iii) The moment a part of the aggregate surface is encountered within a radius l of the particle location, the random walk is terminated. The particle is then moved to the surface (in a sense, “field driven”) and becomes part of the aggregate.

The simulations were stopped when the aggregate had grown to a radius of around 200 units, one unit being the diameter of a single particle. Approximately $10^4 - 10^5$ particles had to be launched for various cases.

The two control parameters employed in this simulation have also been suggested elsewhere in the literature. To model porous silicon formation, a “finite diffusion length” similar to our ΔW has been suggested [17]. The drift length l in our simulation is in a way similar to the width of the “migrational envelope” of Erlebacher *et al.* [14,21]. A depletion layer width ΔW and a drift diffusion length l have been used in conjunction with other parameters to successfully model porous silicon formation [22]. Our algorithm interpolates between existing growth models in various limiting cases. In the limit $l = 1$ and $\Delta W \rightarrow \infty$, the algorithm is identical to the DLA. $\Delta W = 0$ and $l = 1$ approximates the Eden limit. As l becomes larger than ΔW (the case depicted in Fig. 1), a fraction of the generated particles is directly

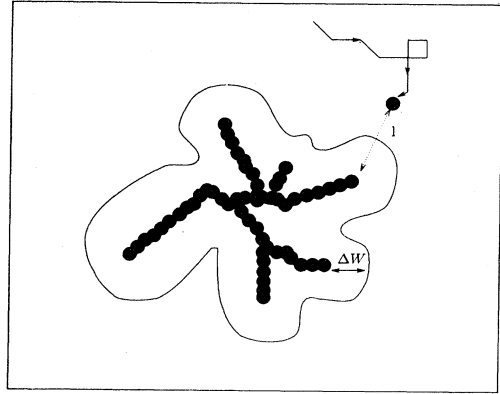


FIG. 1. The drift-diffusion model. A particle is released beyond the depletion layer boundary (the closed curve), which dynamically follows the aggregate (solid circle cluster) contour at a distance ΔW . When the particle wanders to within a radius l (see dotted arrow) of the aggregate surface, it is “field driven” to become a part of the cluster.

transported to the surface without undergoing diffusion. This is akin to ballistic deposition. When $l \gg \Delta W$, the ballistic process dominates the diffusive process.

III. RESULTS

Figure 2 depicts the variety of morphologies obtained with varying ΔW and l . For small $l/\Delta W$, we obtain DLA-like patterns [Fig. 2(a)]. A simple mass-radius scaling calculation for this pattern yielded a fractal dimension of 1.65 ± 0.05 . Stringy structures similar to those

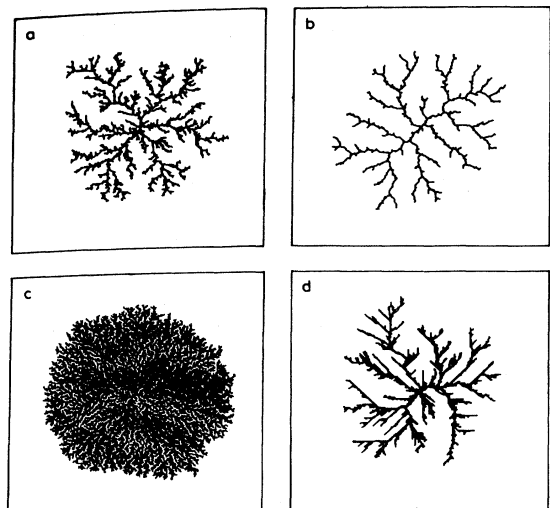


FIG. 2. Map of the simulated growth patterns with varying depletion width ΔW and drift length l . (a) Patterns resembling DLA ($\Delta W = 10$, $l = 2$), (b) stringy structures ($\Delta W = 10$, $l = 10$), (c) homogeneous, dense branching morphologies with a nearly circular growth front ($\Delta W = 2$, $l = 2$) and (d) thick dendritic growth with side branches ($\Delta W = 8$ and $l = 24$).

reported in electrochemical deposition at high voltages [3] are seen in the large ΔW limit with $l/\Delta W \simeq 1$ [Fig. 2(b)]. The mass-radius scaling exponent fluctuates around ~ 1.45 for this pattern. The stringy morphology observed in some experiments is essentially one dimensional in character [4]. This is reproduced for very large $\Delta W (= l) > 25$. As $\Delta W (= l)$ is increased, the scaling exponent approaches unity (see Fig. 4). On the other hand, for small ΔW and $l/\Delta W \simeq 1$, we obtained short dense branches exhibiting a relatively smooth front that remains nearly circular throughout the growth period [Fig. 2(c)]. This has been identified in experimental literature as homogeneous or tip splitting patterns [3,4,7,23]. The mass-radius scaling for these structures resulted in a fractal dimension $\simeq 2$. For $l/\Delta W \geq 3$, thick dendritic growths with side branching were obtained [Fig. 2(d)]. For large $\Delta W (> 5)$, the patterns become too inhomogeneous to show any well defined scaling [3]. However, for small ΔW , the model approaches the Eden limit and the resultant patterns are somewhat homogeneous.

The occurrence of dendritic growth in such a simulation is surprising, since it is well understood that anisotropy is required in the interfacial dynamics for side branching to occur [1]. The present algorithm admits an underlying anisotropy in the way a particular surface site is chosen, when more than one point on the aggregate surface falls within a radius l of the random walker. This selection was done in three ways. (i) The nearest site was chosen. (ii) A site was chosen at random. (iii) The site nearest to the radial line connecting the random walker and the central seed was chosen. The morphologies remained similar for the case $l \leq \Delta W$. The three methods yielded different results in the limit $l \gg \Delta W$. Dendritic growth was observed only in case (iii), which corresponds to the imposition of a preferred radial field. In the case of electrodeposition, this could be interpreted as the applied radial electrostatic field.

Figures 3 and 4 show the variation in the mass-radius scaling exponent d_f with varying values of ΔW and l .

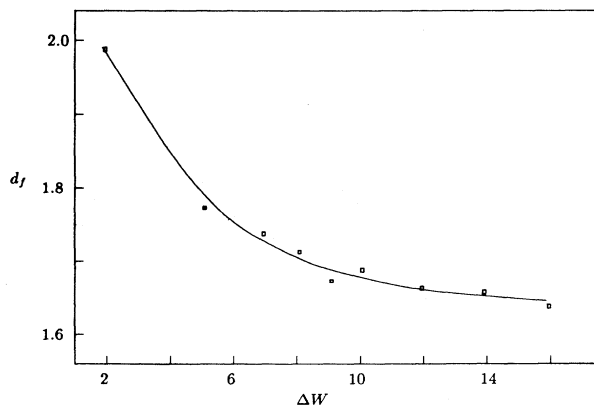


FIG. 3. The fractal dimension d_f plotted against ΔW (in lattice units) with $l = 2$. For small ΔW , $d_f \simeq 2$, which is indicative of compact clusters. In the large ΔW limit, d_f stabilizes at 1.65 ± 0.05 .

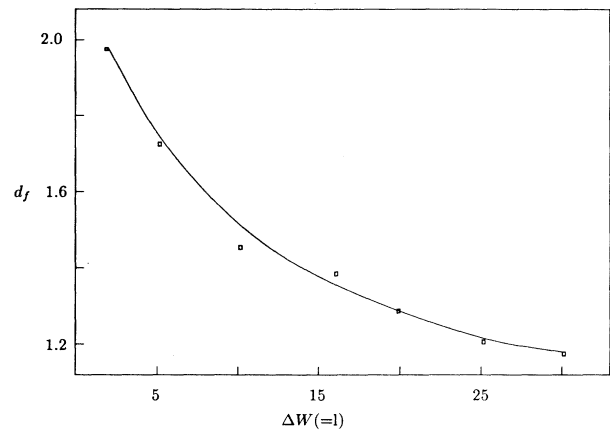


FIG. 4. The fractal dimension d_f plotted against ΔW (in lattice units) with l equal to ΔW . d_f is seen to approach unity in the large $\Delta W (= l)$ limit.

The values obtained for various ΔW when l is kept constant ($l = 2$) are plotted in Fig. 3. d_f is seen to vary from 2.00 to 1.65 ± 0.05 as ΔW goes from very small (~ 1) to large (> 15) values. This illustrates a smooth transition between Eden type growth and DLA. As ΔW is kept equal to l and varied, d_f decreases steadily with increasing $\Delta W (= l)$ and approaches unity. This is depicted in Fig. 4 and represents the emergence of stringy structures as shown in Fig. 2.

Figure 5 codifies our observations into a "phase" [24] plot. The plot was constructed on the basis of approximately a hundred patterns, grown to aggregate diameters of around 400 units. The transitions from one phase to

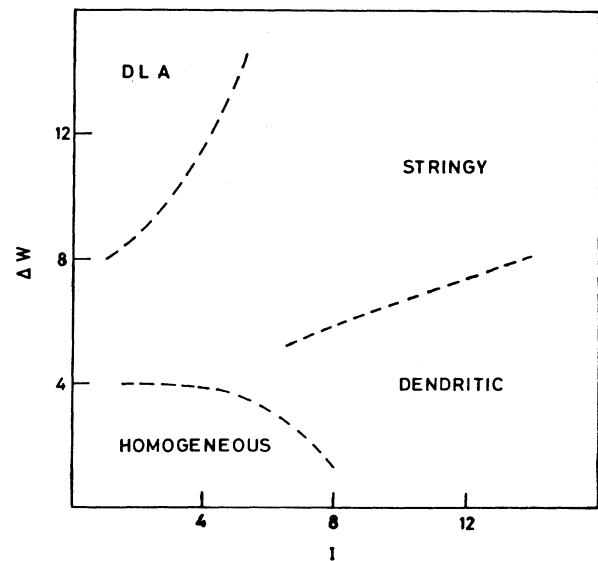


FIG. 5. "Phase" plot of patterns observed in the simulations. The phases depicted transform continuously into one another. Hence, the boundaries must not be treated as rigidly defining a transition. Both ΔW and l are expressed in terms of lattice units.

another being continuous, the boundaries are not rigidly defined. For example, in the $l \gg \Delta W$ case, the dendritic patterns observed at large ΔW become denser and more homogeneous as ΔW approaches zero. The phases depicted have been reported earlier in electrochemical deposition experiments [3,4] and related processes [1].

Several studies of two-dimensional growth on a one-dimensional substrate have been reported in the past. Matsushita, Hayakawa, and Sawada have grown zinc "trees" on a linear carbon cathode [25]. Such processes have also been modeled using a DLA-like algorithm [26]. The etching process in porous silicon may also be viewed similarly [17,21,22]. This is achieved in our model by using a linear substrate that is represented by a side of the lattice. The deposition is no longer radial, but "quasi one dimensional."

Figure 6 depicts the dependence of the mean aggregate density on the drift length l . Deposits were grown on a linear substrate of length 300 units for a given ΔW . A crossover behavior is discernible, with a minimum at $\Delta W = l$. This can be understood in terms of our phase plot (Fig. 5). The minima correspond to the stringy region, where $\Delta W \simeq l$. On either side of the stringy phase, there exists phases of higher density. A similar behavior is seen in porous silicon where transitions are observed from a uniform network of thin pores to shorter, wider pores on increasing the doping level in the substrate [5]. On the other hand, increasing the applied potential leads to the formation of thick and relatively linear pipelike pores [2].

IV. DISCUSSION

The finite diffusion length model of Smith and co-workers is known to exhibit a crossover from fractal to nonfractal clusters when the aggregate size exceeds the diffusion length [18,27]. In our model, a similar behavior is discernible for large aggregate sizes when the simula-

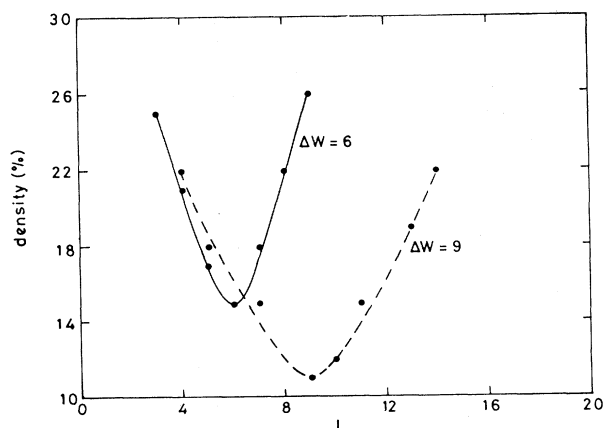


FIG. 6. Plot of the percentage aggregate density vs l (in lattice units) obtained in deposition onto a linear substrate of length 300 units. The two curves are for $\Delta W = 6$ and $\Delta W = 9$. In each case, a minimum is observed at $\Delta W = l$.

tion is carried out for deposition on a linear substrate in a two-dimensional lattice [see Figure 7(a)]. The density decreases with depth and finally becomes almost depth independent. This is indicative of a nonfractal behavior (i.e., in the depth independent region). However, in the case of radial deposition onto a central seed, no such transition was observed for aggregate diameters from 100 to 1000 lattice units. The mass radius scaling exponent remained independent of the aggregate size. This is depicted in Fig. 7(b), which plots the aggregate mass against the cluster radius. The constant slope of the log-log plot is indicative of scale invariance over a large range of diameters (100–1000).

One can explore the phenomenological relevance of the parameters ΔW and l . The significant role played by microscopic dynamics in modifying the solutions of macroscopic analyses has received growing appreciation in the recent past [1]. In the diffusion field versus drift field dynamics governing growth in this simulation, ΔW is

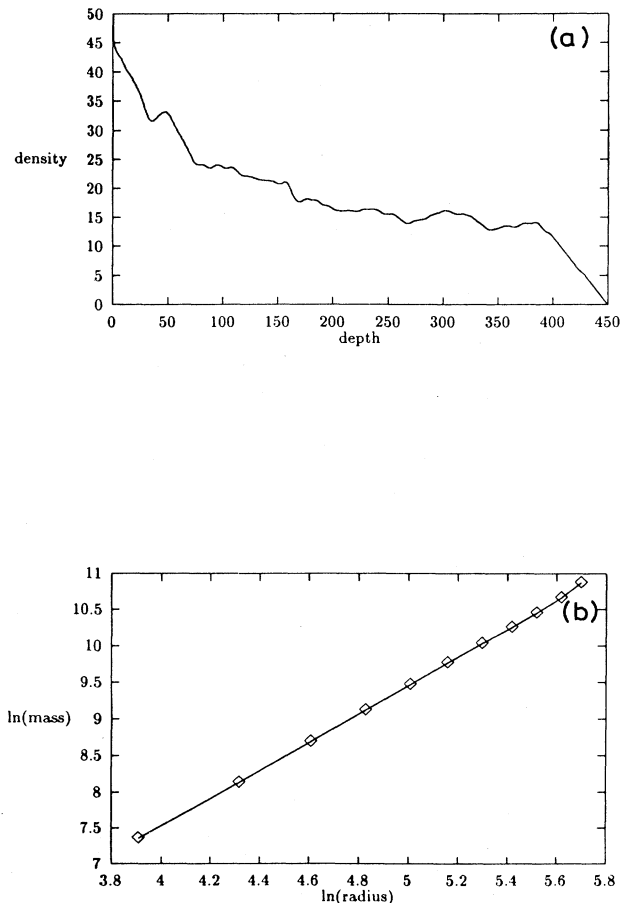


FIG. 7. (a) Percentage aggregate density vs depth (in lattice units) plot for the deposition onto a linear substrate. Simulation is done for a 500×500 lattice with $\Delta W = 5$ and $l = 2$. A crossover to nonfractal behavior where the density is almost depth independent is seen. (b) Log-log plot of the mass vs cluster radius for radial deposition onto a central seed. The clusters are seen to be scale invariant over a large range of diameters (100–1000 lattice units).

a control parameter for the macroscopic diffusion field, whereas l models microscopic surface effects. An example of a phenomenological model employing similar arguments is the Beale model [5] for porous silicon formation, which hypothesizes the existence of a depletion layer whose width varies as

$$\Delta W \propto \left[\frac{(V_{BI} - V_A)}{n_0} \right]^{1/2}, \quad (1)$$

where V_a is the anodization potential, V_{BI} is a constant built-in voltage, and n_0 is the substrate doping level. On the other hand, the parameter l can be related to the barrier lowering ($\Delta\phi_s$) due to microscopic surface irregularities. This lowering $\Delta\phi_s \propto \sqrt{E_s}$, where E_s is the enhanced local electric field. For planar interfaces, $E_s \propto \phi_s/\Delta W$ where ϕ_s is the overall barrier height. Due to surface irregularities, this height is enhanced locally as

$$E_s \propto \frac{\phi_s}{(\Delta W - l)} \quad (l < \Delta W). \quad (2)$$

As $l \rightarrow \Delta W$, E_s is very large at the tips, leading to stringy patterns and the minima in Fig. 6. In a recent work [22], it has been shown that ΔW and l can be correlated to the depletion layer width and barrier lowering given in Eqs. (1) and (2).

The existence of competing processes in electrochemical deposition and other phenomena is well established. The phase diagrams reported by Sawada, Dougherty, and Gollub and Grier *et al.* represents various morphologi-

cal classes resulting from a variation of the concentration and applied voltage. Assigning a direct correlation between our parameters and the experimental parameters based on a comparison between the phase diagrams of the simulation and experiment is difficult. In all probability, ΔW and l are functions of both concentration and applied voltage. Further work needs to be done to establish the exact functional correlations between ΔW and l and the physical processes involved in electrochemical deposition.

In a sense, the two scales ΔW and l are antithetical, one separating the particle from the aggregate, the other driving it towards the aggregate. Various growth models (DLA, ballistic deposition, Eden) can be obtained as limiting cases of this algorithm. We stress that the two scales do not contain any *a priori* bias towards any specific morphological structure. Nevertheless, a variety of distinct morphological structures observed in experimental growth and dissolution is obtained in our simulation.

ACKNOWLEDGMENTS

Useful discussions with Dr. D. Dhar and Dr. D. Chowdhury are gratefully acknowledged. We thank Professor B.M. Arora, SSE group, TIFR where part of the work was carried out. We acknowledge financial support from the Council for Scientific and Industrial Research, and the Department of Science and Technology Government of India.

-
- [1] E. Ben-Jacob and P. Garik, *Nature* **343**, 523 (1990).
 - [2] R.L. Smith and S.D. Collins, *J. Appl. Phys.* **71**, R1 (1992).
 - [3] Y. Sawada, A. Dougherty, and J.P. Gollub, *Phys. Rev. Lett.* **56**, 1260 (1986).
 - [4] D. Grier, E. Ben-Jacob, R. Clarke, and L.M. Sander, *Phys. Rev. Lett.* **56**, 1264 (1986).
 - [5] M.I.J. Beale *et al.*, *J. Cryst. Growth* **73**, 622 (1985).
 - [6] W.W. Mullins and R.F. Sekerka, *J. Appl. Phys.* **34**, 323 (1963).
 - [7] D. G. Grier, D. A. Kessler, and L.M. Sander, *Phys. Rev. Lett.* **59**, 2315 (1987).
 - [8] P. Garik *et al.*, *Phys. Rev. Lett.* **62**, 2703 (1989).
 - [9] H.J. Herrmann, *Phys. Rep.* **136**, 153 (1986).
 - [10] P. Meakin, in *Phase Transitions and Critical Phenomena Vol.12*, edited by C. Domb and T.L. Lebowitz (Academic, New York, 1988).
 - [11] *On Growth and Form*, Vol. 100 of *NATO Advanced Studies Institute Series E: Applied Sciences*, edited by H.E. Stanley and N. Ostrowsky (Martinus Nijhoff, Cargese, France, 1985).
 - [12] T.A. Witten and L.M. Sander, *Phys. Rev. Lett.* **47**, 1400 (1981).
 - [13] T. Vicsek, *Phys. Rev. Lett.* **53**, 2281 (1984).
 - [14] J. Erlebacher, P.C. Searson, and K. Sieradzki, *Phys. Rev. Lett.* **71**, 3311 (1993).
 - [15] O. Shochet *et al.*, *Physica A* **181**, 136 (1992).
 - [16] O. Shochet *et al.*, *Physica A* **187**, 87 (1992).
 - [17] R.L. Smith, S.-F. Chuang, and S.D. Collins, *J. Electron. Mater.* **17**, 533 (1988).
 - [18] R.L. Smith and S.D. Collins, *Phys. Rev. A* **39**, 5409 (1989).
 - [19] R.F. Voss, *J. Stat. Phys.* **36**, 861 (1984).
 - [20] R.C. Ball and R.M. Brady, *J. Phys. A* **18**, L809 (1985).
 - [21] J. Erlebacher, K. Sieradzki, and P.C. Searson, *J. Appl. Phys.* **76**, 182 (1994).
 - [22] G.C. John and V.A. Singh, *Phys. Rev. B* **52**, 11125 (1995).
 - [23] E. Ben-Jacob *et al.*, *Phys. Rev. Lett.* **57**, 1903 (1986).
 - [24] The term "phases" is taken to mean classes of aggregates as reported earlier in literature.
 - [25] M. Matsushita, Y. Hayakawa, and Y. Sawada, *Phys. Rev. A* **32**, 3814 (1985).
 - [26] P. Meakin, *Phys. Rev. A* **27**, 2616 (1983).
 - [27] R.W. Bower and S.D. Collins, *Phys. Rev. A* **43**, 3165 (1991).